Dear Editor,

Thank you very much for reviewing our paper “**Low-latitude climate change linked to high-latitude glaciation during the Late Palaeozoic Ice Age: evidence from the terrigenous detrital kaolinite**" and giving very valuable comments. The points raised are valid so the review provides us with the opportunity to expand our manuscript to address them comprehensively. Below we address each point individually and consider them fully resolved.

In the submission system, we cannot upload the revised manuscript. Therefore, we outline the changes we have made as indicated on the updated version of the manuscript showing marked changes (in red) as an attachment here.

We hope you find these changes agreeable and we look forwards to hearing from you in the future.

Yours sincerely and on behalf of co-authors,

Jason Hilton

Reviewer #2:

Overall, reviewer 2 makes some detailed comments on the geological context of the study but nothing that impacts the results or conclusions presented. We will reply to their comments individually below.

1. The paleogeographic context is inadequate. Fig. 1a is a cartoon with virtually no documentation of how the North China Block was positioned in the Early Permian, e.g., Liu1990 cited is a one-page comment/reply and Blakely2011 has no quantitative analysis for determination of paleolatitude, whereas Yang+Lei1987 and Zhou2002 are not readily accessible and would need to be described here for a broader audience. The authors state that the NCP was located at ~5-15°N but there could be a huge lithostratigraphic consequence between being in the tropical humid belt (5°) and the arid belt (15°). Unless the authors have alternative methods, paleolatitudes are based on paleomagnetism and hence the authors might consult references to the modern paleomagnetic literature and syntheses for the NCB and Tethyan environs in papers like Torsvik+2012 ESR or Kent+Muttoni2020 Palaeo3.

Response: We disagree with the overall sentiment here – the information is provided is coparable to other papers on the topic utilizing similar apprаches, but if the reviewer wants us to provide additional context, we can do that. We note this does not change the results or conclusions presented.

We have reviewed palaeomagnetic data from the Dafengkou section in the Yuzhou coalfield from the early to late Early Permian (including the Taiyuan, Shanxi, and Shangshihezi formations). These data show that from the early Early Permian to late Early Permian, the palaeolatitude change in the study area is between 11.0°N and 11.4°N, that is, it is within the equatorial humid climate zone (Zhu et al., 1996).

Table 1 The Characteristic remanent magnetization directions, palaeomagnetic pole, and palaeolatitude of Permian of Dafengkou profile in Yuzhou, Henan Province

Period	sampling point	mean direction of magnetization			α95	stability valuation	Palaeomagnetic pole position				Palaeolatitude position
		D (°)	I (°)	K (°)			Plat.(°N)	Plong.(°N)	Dp	Dm	
P^2_1	6	143.2	-21.2	12.9	19.4	R	-49.2	177.4	10.7	20.4	11.0
P^1_1	3	124.9	-22.0	82.1	13.7	R	-35.1	192.5	7.7	14.5	11.4
P_1	9	136.9	-21.7	16.1	13.2		-44.6	183.4	7.4	14.0	11.2

According to palaeomagnetic data from the Dafengkou section in the Yuzhou Coalfield during the early Early Permian (P_1) to late Early Permian ($P^2{}_1$) (Table 1; see below), we determined the exact location of the study area through time and have modified this in the geological background section. We have revised figure 1, and replaced “Blake’s paleogeographic map (Fig. 1a)” with the “generalized tectonic map of present-day China”, and also replaced the “Palaeofacies map of the NCP during the Cisuralian (modified from Liu, 1990) (Fig. 1b)” with the “Simplified tectonic map of the present-day NCP (modified from Liu et al., 2013)”. In these maps, we have added modern latitude and longitude (Figs. 1a, 1b; see below). However, this information does not affect the geological background in our manuscript. We have added a map of the the facies and palaeogeographic evolution of the NCP over time from the late Bashkirian to the Wordian (~318 Ma – 265.1 Ma) in the revised manuscript (Figure 9) to provde full context on this.

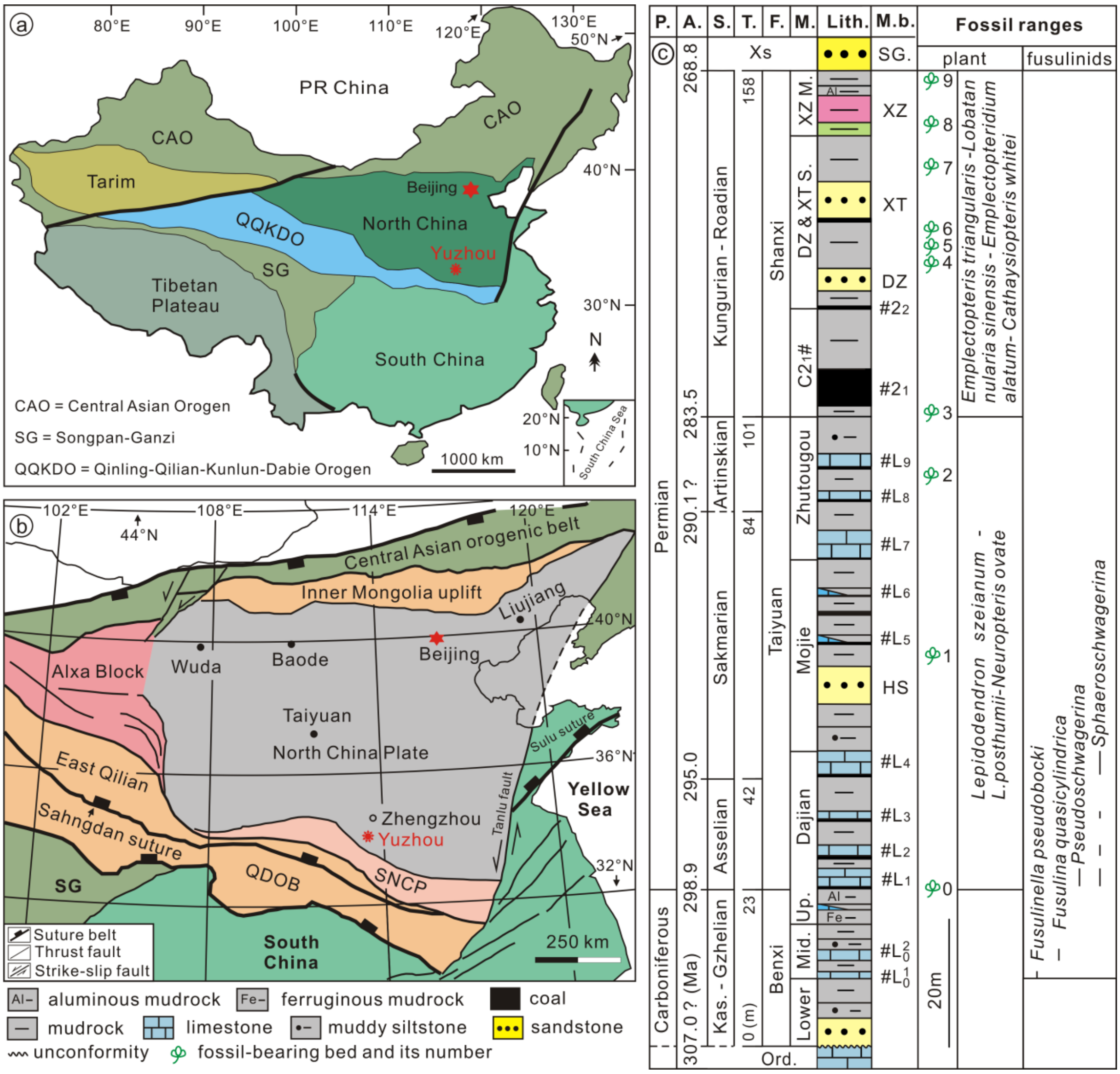

Figure 1. Location and geological context for the study area. **a**, Generalized tectonic map of present-day China showing the location of the North China Plate (NCP) and the study area (modified from Lu et al., 2020); **b**, Simplified tectonic map of the present-day NCP showing the location of the study area (modified from Liu et al., 2013). **c**, Stratigraphic framework and fossil distributions for the studied Carboniferous-Permian strata of the Benxi, Taiyuan, Shanxi, and Xiashihezi (Xs) formations from Henan Province in the southern NCP. Lithology column derived from Pei (2004) and Yang (2006) with colors representing those of the strata in the field (section 2). L_0^1 to L_9 represent the position of individual limestone marker beds. Fossil plant assemblages (0–9) from Yang (2006) and Yang and Wang (2012). Fusulinid stratigraphic ranges and biozones from Pei (2004, 2009). Abbreviations: SG = Songpan-Ganzi Terrane; QDOB = Qingling-Dabie orogenic belt; SNCP = south North China Plate; P. = Period; S. = Stages; Ord. = Ordovician; Kas. = Kasimovian; T. = Cumulative thickness; F. = Formation; M. = Member; $C2_1$# = Coal 2_1 seam Member; DZ & XT S. = Dazhan and Xiangtan Sandstone Member; XZ M. = Xiaozi Mudrock Member; Mid. = Middle; Up. = Upper; Lith. = Lithology; M.b. = Marker bed; HS= Hushi sandstone; 2_1# = Coal 2_1 seam; DZ = Dazhan sandstone; XT = Xiangtan sandstone; XZ = Xiaozi mudrock; SG. = Shaguoyao sandstone.

2. There is a bewildering array of regional and global stage names and fossil zonations for the Late Paleozoic but one would have to be a real aficionado to decipher from Fig. 1c where in the geologic column all the names are supposed to be: Early Permian? A very rudimentary paleogepographic map (Fig. 1b), which should at least show lines of paleolatitude, is labeled Cisuralian but that time-stratigraphic interval is not indicated in the stratigraphic column in Fig. 1b.

Response: We have added the names of geological periods (e.g., Carboniferous and Permian) in the geological column in Figure 1c (Fig. 1c; see Response 1). We have replaced the "Palaeofacies map of the NCP during the Cisuralian (modified from Liu, 1990)(Fig. 1b)" with a"Simplified tectonic map of the present-day NCP showing the location of the study area (modified from Liu et al., 2013)", but this did not affect the geological background in our manuscript. We have also added a map of the evolution of the NCP (see above) over time from late Bashkirian to Wordian (~318 Ma – 265.1 Ma) in the manuscript (Figure 9), and added the paleolatitude based on the previous palaeomagnetic data (Zhu et al., 1996; Table 1).

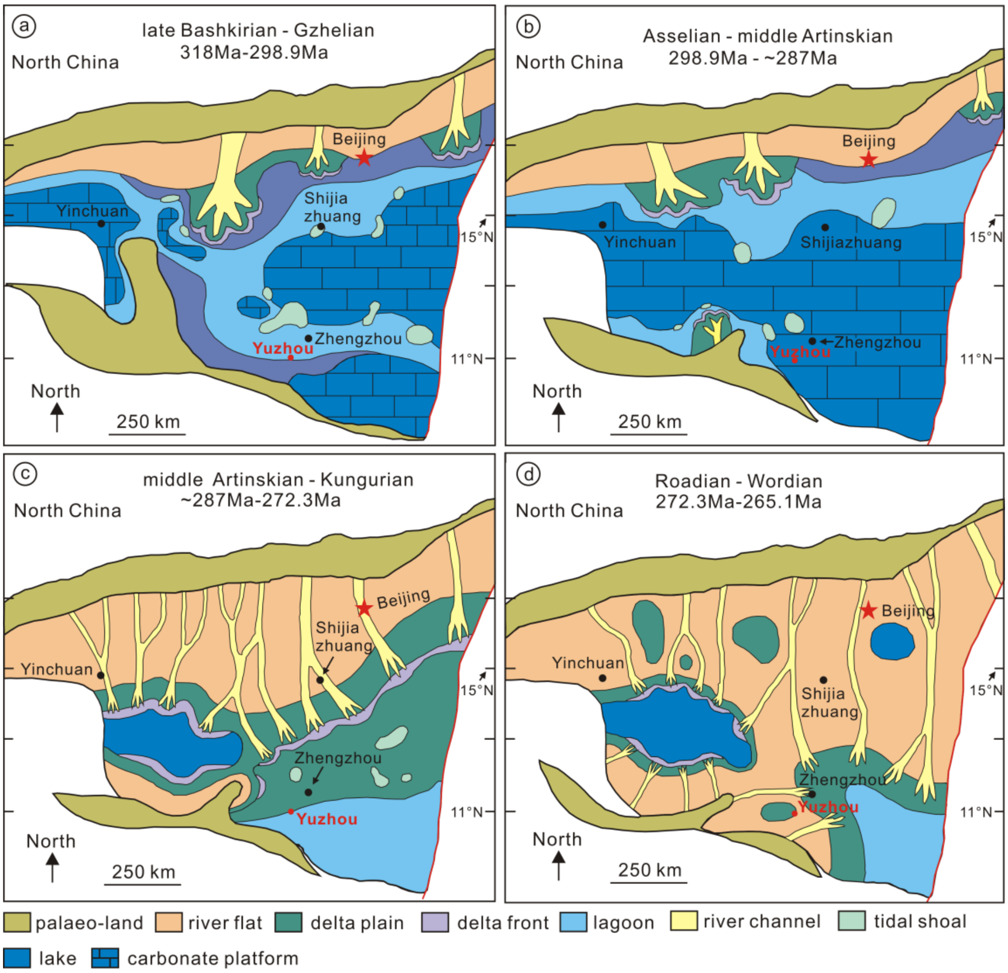

Figure 9. Lithofacies palaeogeograpy map from late Bashkirian (Carboniferous) to Wordian (Permian) in the North China Plate (modified from Shao et al., 2014). Note palaeolatitude is derived from palaeomagnetic data in Table 1 (Zhu et al., 1996).

3. Two U-Pb dates are quoted as 270.7 Ma and 299.4 Ma based on 5-11 zircons selected from an astonishing number (1000 to 1500!) grains extracted from two levels. The technique is not described (presumably laser-ablation ICPMS) nor how the 1:100 grains were selected, or what was done with the remaining zircon grains (were they measured?). What about potential lead-loss? These dates are extremely important for the chronostratigraphy and correlation to the wider world and must be described in much more detail; the reportage of Gehrels+2020 Geochro may provide a useful example.

Response: We previously cited a paper that used exactly the same protocols, but we have now added a description of the zircon U-Pb dating analysis method in the text (see below).

The diameters of all zircon cystals in both ash beds (HYD-1 and HYD-2) were measured, with crystal sizes ranging from 50 to 200 μm. Due to the fact that 1 epoxy mount is limited to 100 zircons, so we randomly selected 100 out of 1000 and 1500 zircon grains in HYD-1 and HYD-2, respectively. Then we randomly selected 50 out of these 100 zircon grains in epoxy mount for analysis. In the HYD-1 zircon sample, the ages of 23 out of 50 zircon grains are invalid (no data). In the remaining 27 zircon grains, 2 zircon grains have concordance degrees below 90%, while the remainder has concordance degrees above 90% (Table S2). In the HYD-2 zircon sample, the ages of 32 out of 50 zircon grains are invalid (no data). In the remaining 18 zircon grains, 2 zircon grains have degrees below 90%, while the remainder have concordance degrees above 90% (Table S2). In this study, sedimentary age interpretations are based on the main clusters of youngest zircon ages (there are 11 and 5 youngest zircon ages from the sample HYD-1 and HYD-2, respectively) with a concordance degree greater than 90%, and there is less emphasis on ages with a concordance degree greater than 90% that do not belong to youngest clusters given the possibility that they are unreliable due to Pb loss, inheritance, analysis of inclusions, high common Pb, or unusual Pb–U fractionation due to ablation along with fractures (e.g., Gehrels, 2014; Gehrels et al., 2020).

We have revised the text in the manuscript to read: "After crushing, grinding, sieving, and heavy liquid and magnetic separation, euhedral zircon crystals with clear oscillatory zoning under cathodoluminescence (CL) microscope were selected for U-Pb zircon isotope analysis. U-Pb dating was conducted at the State Key Laboratory of Geological Processes and Mineral Resources, China University of Geosciences (Beijing). Laser sampling was performed using a Coherent's GeoLasPro-193nm system. A Thermo Fisher's X-Series 2 ICP-MS instrument was used to acquire ion-signal intensities. Helium was applied as a carrier gas. Argon was used as the make-up gas and mixed with the carrier gas. All data were acquired on zircon in single spot ablation mode at a spot size of 32 μm with 6 Hz frequency in this study. Standard material SRM610 from National Institute of Standards and Technology (NIST) of America was used to optimize the ICP-MS instrument, and as an external standard for determination of trace elements. Zircon 91500 was used as an external standard for U-Th-Pb isotopic ratios (Wiedenbeck et al., 1995, 2004). Plešovice Zircon was used as a monitoring standard for each analysis (Sláma et al., 2008). Time-dependent drifts of U-Th-Pb isotopic ratios were corrected using a linear interpolation (with time) for every five analyses according to the variations of 91500 (i.e., 2 zircon 91500 + 5 samples + 2 zircon 91500). Each analysis incorporated a background acquisition of approximately 20s (gas blank) followed by 50s data acquisition from the sample. Off-line selection and integration of background and analyte signals, and time-drift correction and quantitative calibration for trace element analyses and U-Pb dating were performed by ICPMSDataCal (Liu et al., 2008). Data reduction and concordia diagram was carried out using the Isoplot 3.0 (e.g., Lu et al., 2021a, b)".

and

"In this study, zircon U-Pb age distributions are displayed and analyzed with probability density diagram, which is based on the individual ages and measured uncertainties from each sample (Fig. 3; Table S2). Sedimentary age interpretations are based on the main clusters of youngest zircon ages, with less emphasis on ages that do not belong to youngest clusters given the possibility that they are unreliable due to Pb loss, inheritance, analysis of inclusions, high common Pb, or unusual Pb–U fractionation due to ablation along with fractures (e.g., Gehrels, 2014; Gehrels et al., 2020)".

4. A thickness-age plot (with cumulative thickness scales and not simply scale also shown in the stratigraphic diagrams in Figs. 1c, 4, 8,) would be useful to access temporal resolution of stages and fossil zonations.

Response: We revised Figure 1c (see Response 1), 4 and 8 (see below), and added the cumulative thickness of the sedimentary stratigraphic time stages.

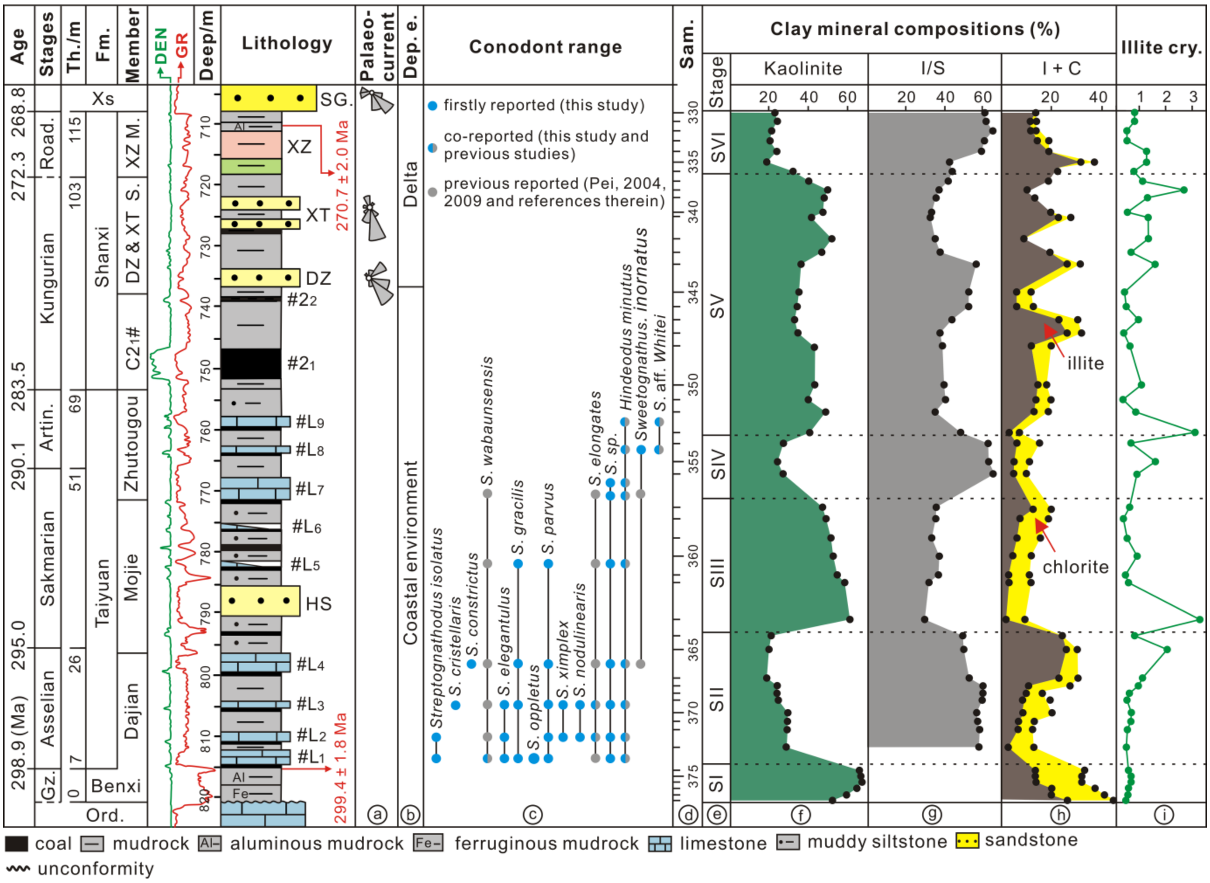

Figure 4. Results from zircon U–Pb dating, conodont biostratigraphic ranges, clay mineral compositions, and illite crystallization from the Yuzhou Coalfield. Colors in the lithology column represent those seen in the field. Bed numbers #L_1-L_9 refer to individual limestone horizons (Pei, 2004). Palaeocurrent data from the Yuzhou Coalfield refer to those of Yang and Lei (1987) reveal that the palaeoflow flowed from north to south in the Shanxi Formation. Interpretation of deposition environments follows Liu (1987) and Yang and Lei (1987). Abbreviations: Th./m = Cumulative thickness /m; Fm. = Formation; Ord. = Ordovician; Gz. = Gzhelian; C2_1# = Coal 2_1 seam Member; DZ & XT S. = Dazhan and Xiangtan Sandstone Member; XZ M. = Xiaozi Mudrock Member; Dep. e. = Depositional environment; HS= Hushi sandstone; #2_1 = Coal 2_1 seam; #2_2 = Coal 2_2 seam; DZ = Dazhan sandstone; XT = Xiangtan sandstone; XZ = Xiaozi mudrock; SG. = Shaguoyao sandstone; Sam. = Sample number; I/S = illite-smectite mixed layers; I+C = illite + chlorite; Illite cry. = illite crystallinity.

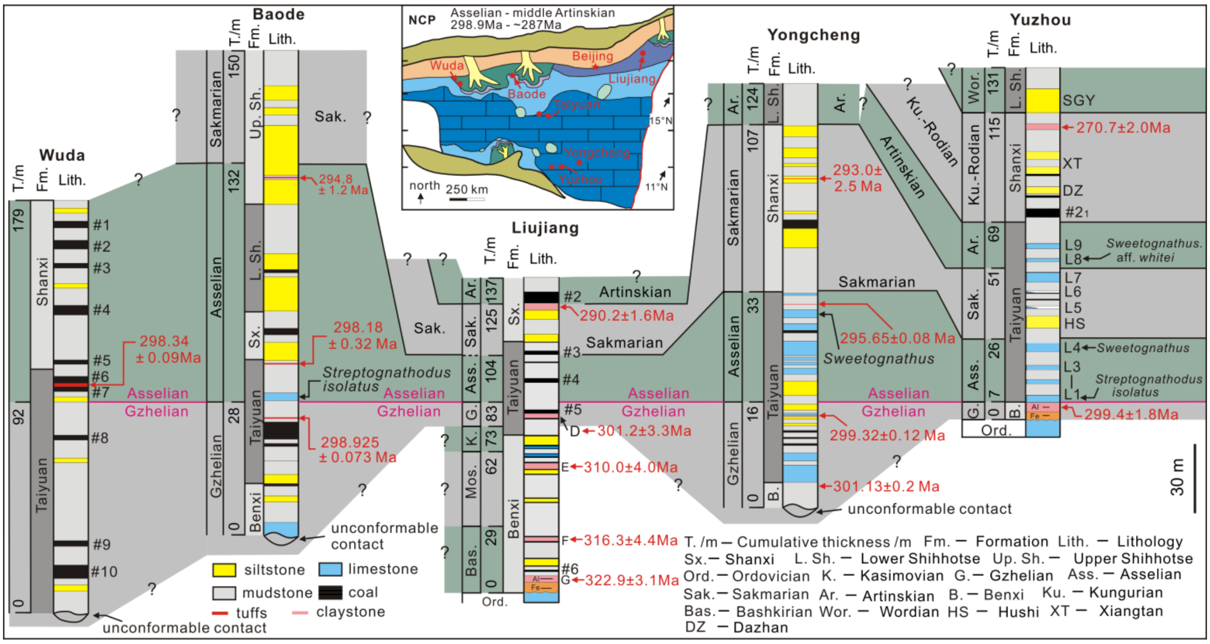

Figure 8. Chronostratigraphic and lithostratigraphic correlation of Carboniferous and Permian in the NCP. Lithology and age data of the sections at Wuda (Zhou et al., 2015 and Schmitz et al., 2020), Baode (Wu et al., 2021), Liujiang (Lu et al., 2021a and Unpublished data), Yongcheng (Yang et al., 2020), and Yuzhou (this study) organized from north to south on the NCP during the Late Pennsylvanian to the earliest Guadalupian. Note lithofacies palaeogeograpy map from Asselian to middle Artinskian in the NCP showing the location of the chronostratigraphic and lithostratigraphic correlation section (modified from Shao et al., 2014). Palaeolatitude is derived from palaeomagnetic data (Zhu et al., 1996; Table 1).

Reference:

Gehrels, G.: Detrital Zircon U-Pb Geochronology Applied to Tectonics, Annu. Rev. Earth Planet. Sci., 42(1), 127–149, doi:10.1146/annurev-earth-050212-124012, 2014.

Gehrels, G., Giesler, D., Olsen, P., Kent, D., Marsh, A., Parker, W., Rasmussen, C., Mundil, R., Irmis, R., Geissman, J. and Lepre, C.: LA-ICPMS U–Pb geochronology of detrital zircon grains from the Coconino, Moenkopi, and Chinle formations in the Petrified Forest National Park (Arizona), Geochronology, 2(2), 257–282, doi:10.5194/gchron-2-257-2020, 2020.

Liu, G. H., 1987. The features and types of the late Carboniferous carbonate tempestites in the Dafengkou area, Yuxian, Western Henan. Geol. Rev., 33, 249–257, 1987.

Liu, Y., Hu, Z., Gao, S., Günther, D., Xu, J., Gao, C. and Chen, H.: In situ analysis of major and trace elements of anhydrous minerals by LA-ICP-MS without applying an internal standard, Chem. Geol., 257(1–2), 34–43, doi:10.1016/j.chemgeo.2008.08.004, 2008.

Liu, S., Su, S. and Zhang, G.: Early Mesozoic basin development in North China: Indications of cratonic deformation, J. Asian Earth Sci., 62, 221–236, doi:10.1016/j.jseaes.2012.09.011, 2013.

Lu, J., Zhang, P., Yang, M., Shao, L. and Hilton, J.: Continental records of organic carbon isotopic composition ($\delta^{13}C_{org}$), weathering, paleoclimate and wildfire linked to the End-Permian Mass Extinction. Chem. Geol., 558, 119764. doi: 10.1016/j.chemgeo.2020.119764, 2020.

Lu, J., Wang, Y., Yang, M., Shao, L. and Hilton, J.: Records of volcanism and organic carbon isotopic composition (δ13Corg) linked to changes in atmospheric pCO2 and climate during

the Pennsylvanian icehouse interval. Chem. Geol., 570, 120168. doi: 10.1016/j.chemgeo.2021.120168, 2021a.
Lu, J., Zhang, P., Dal Corso, J., Yang, M., Wignall, P. B., Greene, S. E., Shao, L., Lyu, D. and Hilton, J.: Volcanically driven lacustrine ecosystem changes during the Carnian Pluvial Episode (Late Triassic), Proc. Natl. Acad. Sci. (U.S.A.), 118(40), e2109895118, doi:10.1073/pnas.2109895118, 2021b.
Pei, F.: The North China type Permo-Carboniferous fusulinid and conodont biostratigraphic units of Henan Province. J. Stratigr., 28, 344–353. doi: 10.3969/j.issn.0253-4959.2004.04.011, 2004.
Pei, F.: Stratigraphic subdivision and chronological correlation of the North China-type Permo-Carboniferous in Henan. Acta Geol. Sin. Henan, 21–33, 2009.
Schmitz, M. D., Pfefferkorn, H. W., Shen, S. Z. and Wang, J.: A volcanic tuff near the Carboniferous–Permian boundary, Taiyuan Formation, North China: Radioisotopic dating and global correlation. Rev. Palaeobot. Palynol., 104244. doi:10.1016/j.revpalbo.2020.104244, 2020.
Shao, L., Dong, D., Li, M., Wang, H., Wang, D., Lu, J., Zheng, M. and Cheng, A.: Sequence-paleogeography and coal accumulation of the Carboniferous-Permian in the North China Basin, J. China. Coal. Soc., 39(8), 1725–1734, doi:10.13225/j.cnki.jccs.2013.9033, 2014.
Sláma, J., Košler, J., Condon, D. J., Crowley, J. L., Gerdes, A., Hanchar, J. M., Horstwood, M. S. A., Morris, G. A., Nasdala, L., Norberg, N., Schaltegger, U., Schoene, B., Tubrett, M. N. and Whitehouse, M. J.: Plešovice zircon — A new natural reference material for U–Pb and Hf isotopic microanalysis, Chem. Geol., 249(1–2), 1–35, doi:10.1016/j.chemgeo.2007.11.005, 2008.
Wiedenbeck, M., Alle, P., Corfu, F., Griffin, W. L., Meier, M., Oberli, F. v, Quadt, A. von, Roddick, J. C. and Spiegel, W.: Three natural zircon standards for U-Th-Pb, Lu-Hf, trace element and REE analyses, Geostand. Newsl., 19(1), 1–23, doi:10.1111/j.1751-908X.1995.tb00147.x, 1995.
Wiedenbeck, M., Hanchar, J. M., Peck, W. H., Sylvester, P., Valley, J., Whitehouse, M., Kronz, A., Morishita, Y., Nasdala, L., Fiebig, J., Franchi, I., Girard, J.-P., Greenwood, R. C., Hinton, R., Kita, N., Mason, P. R. D., Norman, M., Ogasawara, M., Piccoli, P. M., Rhede, D., Satoh, H., Schulz-Dobrick, B., Skår, O., Spicuzza, M., Terada, K., Tindle, A., Togashi, S., Vennemann, T., Xie, Q. and Zheng, Y.-F.: Further Characterisation of the 91500 Zircon Crystal, Geostand. Geoanalytical Res., 28(1), 9–39, doi:10.1111/j.1751-908X.2004.tb01041.x, 2004.
Wu, Q., Ramezani, J., Zhang, H., Wang, J., Zeng, F., Zhang, Y., Liu, F., Chen, J., Cai, Y., Hou, Z., Liu, C., Yang, W., Henderson, C. M. and Shen, S.: High-precision U-Pb age constraints on the Permian floral turnovers, paleoclimate change, and tectonics of the North China block. Geology, 49, 677-681. doi: 10.1130/G48051.1, 2021.
Yang, G. X.: The Permian Cathaysian Flora in Western Henan province, China - Yuzhou Flora. Geological Publishing House, Beijing, pp. 1–76, 2006.
Yang, G. X., Wang, H. S.: Yuzhou flora - a hidden gem of the Middle and Late Cathaysian Flora. Sci. China Earth Sci., 55, 1601–1619. doi: 10.1007/s11430-012-4476-2, 2012.
Yang, Q. and Lei, S.: Depositional environments and coal-forming characteristics of Late Palaeozoic Coal Measures in Yuxian, Henan Province. Geological Publishing House, Beijing, pp. 1–87, 1987.
Yang, J. H., Cawood, P. A., Montañez, I. P., Condon, D. J., Du, Y. S., Yan, J. X., Yan, S. Q. and Yuan, D. X.: Enhanced continental weathering and large igneous province induced climate

warming at the Permo-Carboniferous transition. Earth Planet. Sci. Lett., 534, 116074. doi: 10.1016/j.epsl.2020.116074, 2020.

Zhu, H., Yang, G. and Sheng, A. X.: A study on palaeomagnetism of Permian strata in the Dafengkou section, Yuzhou, Henan Province, Acta Geol. Sin., 70(2), 121–128, 1996.

Zhou, W. M., Wan, M. L., Yan, M. X., Cheng, C. and Wang, J.: The succession sequence of early Permian wetland vegetational communities in the Shanxi Formation of the Wuda Coalfield, Inner Mongolia. Acta Palaeontol. Sin., 54, 66-83. doi: CNKI:SUN:GSWX.0.2015-01-005, 2015.